Vector Magnetic Fields, Subsurface Stresses and Evolution of Magnetic Helicity

Richard Canfield* & Alexei Pevtsov, *Department of Physics, Montana State University, Bozeman, Montana 59717–3840.*
email: canfield@physics.montana. Edu

Abstract. Observations of the strength and spatial distribution of vector magnetic fields in active regions have revealed several fundamental properties of the twist of their magnetic fields. First, the handedness of this twist obeys a hemispheric rule: left-handed in the northern hemisphere, right-handed in the southern. Second, the rule is weak; active regions often disobey it. It is statistically valid only in a large ensemble. Third, the rule itself, and the amplitude of the scatter about the rule, are quantitatively consistent with twisting of fields by turbulence as flux tubes buoy up through the convection zone. Fourth, there is considerable spatial variation of twist within active regions. However, relaxation to a linear force-free state, which has been documented amply in laboratory plasmas, is not observed.

Key words. Magnetic fields—currents—magnetic helicity.

1. Introduction

The magnetic fields of the Sun and stars are believed to be produced by dynamos, whose physical nature is one of the most interesting topics of modern solar and stellar research. The last two decades have seen dramatic advances in our knowledge of how such dynamos work. It is now widely believed that the solar dynamo is located at the radial shear zone revealed by helioseismology near the base of the convection zone. Magnetic flux generated there is buoyant and rises through the convection zone as Ω-loops, whose ends are anchored in the convectively stable core. Great progress has been made in understanding flux emergence processes (e.g., Spruit 1981, Chou & Fisher 1989; D'Silva & Choudhuri 1993; Fan, Fisher & McClymont 1994; Caligari, MorenoInsertis & Schüssler 1995). Observational data have been matched accurately by nonlinear models of thin magnetic flux tubes rising buoyantly to the solar surface (D'Silva & Choudhuri 1993, Fan, Fisher & McClymont 1994). These models, and their comparison to observed active region data, provide the most compelling evidence that flux does indeed originate beneath the convection zone. Many observed attributes of solar activity may ultimately be understood in terms of either dynamo processes or flux transport processes, or both.

2. Measures of helicity

Before proceeding further, it is appropriate to formally define various quantities relevant to magnetic helicity, including those that can be measured. Consider a magnetic field $B(x) = \nabla \times A(x)$ in a domain D on whose surface $n \cdot B = 0$. The magnetic helicity H of this flux system is then $H = \int_D A \cdot B \, dV$. Consider a thin tube T with local $B(r,\theta,z)$ defined by its axial component $B_a = (0,0,B_z(r))$ and meridional component $B_m = (0, B_\theta(r),0)$. Moffatt & Ricca (1992) showed that the total magnetic helicity H is given by $H = \int_T A_a \cdot B_a \, dV + 2 \int_T A_m \cdot B_m \, dV$. The axial term gives the *writhe* contribution $W = \int_T A_a \cdot B_a \, dV$, and the meridional term gives the *twist* contribution $T = 2\int_T A_m \cdot B_m \, dV$, where $B_a = \nabla \times A_a$ and $B_m = \nabla \times A_m$. Twist and writhe are illustrated in Fig. 1.

We *cannot* observe a full flux system D of an active region, since it extends below the visible surface, so we cannot observationally determine H W, or T. We *can* measure local values of quantities that contribute to the integrand $A \cdot B$. Using vector magnetograms, we determine the photospheric vertical current density j_z over a horizontal area S: $j_z = (\mu_0 S)_{-1} \oint B \cdot d\ell = \mu_o^{-1} (\nabla \times B)_z$. For a force-free field $(\nabla \times B)_z = (\alpha B)_z = \mu_0 j_z$. For a linear (constant–α) force-free field $A \cdot B = \alpha^{-1} B^2$. We use the force-free field parameter α to describe our data, since it can be derived
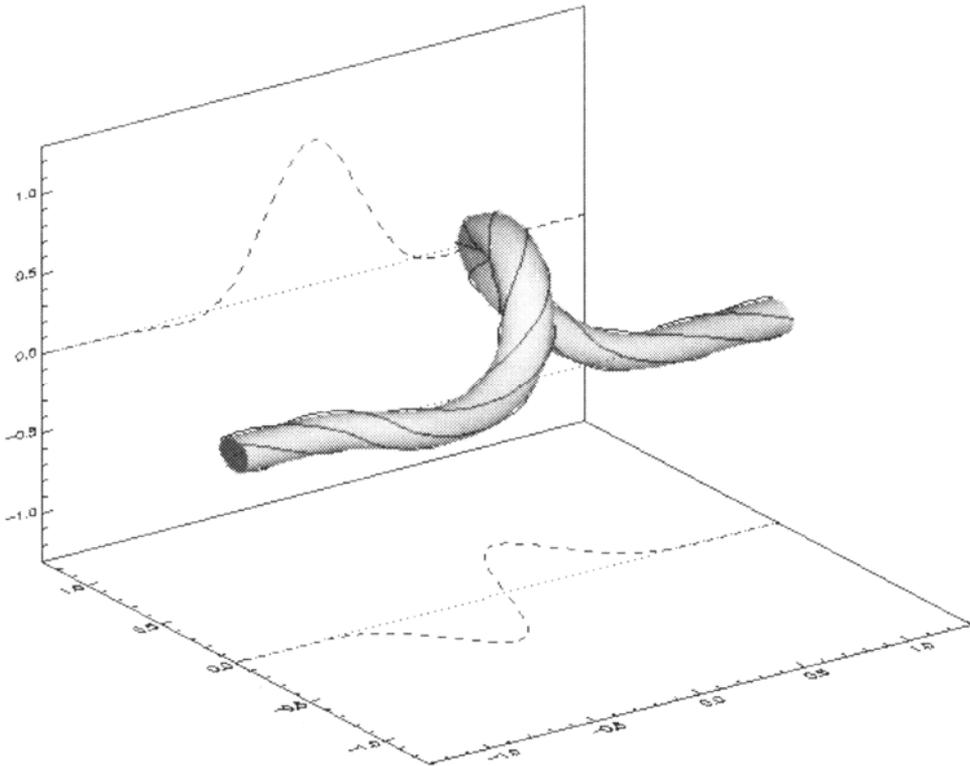

Figure 1. A section of a flux tube with local contributions to twist (right-handed) and writhe (left-handed), defined in section 2.

from observations whether B is force free or not, and it is a local measure of the integrand of *H* if B is force-free, as in the Sun's corona.

The magnetic vector potential A(x) cannot be derived from photospheric vector magnetograms, but both the current helicity ($h_c \equiv$ B$\cdot\nabla \times$ B) and the parameter α can be. The quantities *H, h_c,* and α are related: for a force-free model, for example, *H,* and h_c are proportional to the magnetic energy density and α . The sign of α is a measure of the handedness (chirality) of the field; $\alpha > 0$ for right-handed fields. The nonlocal quantity *H* is conserved in ideal MHD, and nearly so in circumstances relevant to the Sun, when a suitably defined relative helicity is used (Berger 1999). On the other hand, the local quantity h_c is not conserved. It is important to recognize that although h_c is not conserved, it is observed, and can be related to the physics of the convection zone and the dynamo through modeling.

3. Vector magnetic fields and subsurface stresses

Pevtsov, Canfield & Metcalf (PCM, 1995), introduced α_{best} as a quantitative measure of the magnetic field line twist at the photospheric level. This least-squares best-fit value quantifies the amount of twist in the active region as a whole. Independent evidence (Leka *et al.* 1996) suggests that the photospheric twist is a characteristic of the field *prior* to its emergence.

A data set has been compiled of α_{best} measured for 203 different active regions over the period 1991–1995 (Longcope, Fisher & Pevtsov (1998), see Fig. 2). Many of the active regions were observed repeatedly, each observation providing an independent measurement of α_{best}. This offers an estimate of the error in the measured value. Fig. 2 shows point-to-point scatter much greater than the error bars. There is, however, a tendency for α_{best} to vary with latitude; this tendency is statistically significant. The unique strength of these data is their quantitative basis.

Until recently, models of the rise of flux tubes through the convection zone assumed the magnetic field within the tube to be *untwisted,* contrary to this observational evidence. Longcope & Klapper (1997) formulated a model for the dynamics of a twisted thin flux tube. These equations provide the basic theoretical tool necessary to understand the introduction of twist during flux tube rise.

The first application of the Longcope-Klapper equations to a rising magnetic flux tube have yielded a very promising comparison to the PCM dataset (Longcope *et al.* 1998). During its rise the axis of the flux tube is distorted into a sinuous shape by turbulent convective flows. The turbulence is influenced by the Coriolis force, which endows it with kinetic helicity. As a result, the sinuous distortions to the rising flux tube have a slightly helical nature, contributing writhe. The Longcope-Klapper equations describe how these helical (writhing) distortions twist the magnetic field within the tube; they term this coupling between writhe and twist the Σ-*effect.*

The sense of twist within the flux tube is *opposite* to the sense of the helical distortions to the axis. The internal twist therefore has the same handedness as the turbulence. This is opposite to the sign of the well-known α-effect of Parker (1955) and Steenbeck & Krause (1966). Monte Carlo simulations of the Σ-effect compare remarkably well to the data (Fig. 2). There is a statistical trend with the correct sign and latitudinal dependence (solid line). On top of this trend there is substantial statistical scatter (dashed lines) in good quantitative agreement with observations.
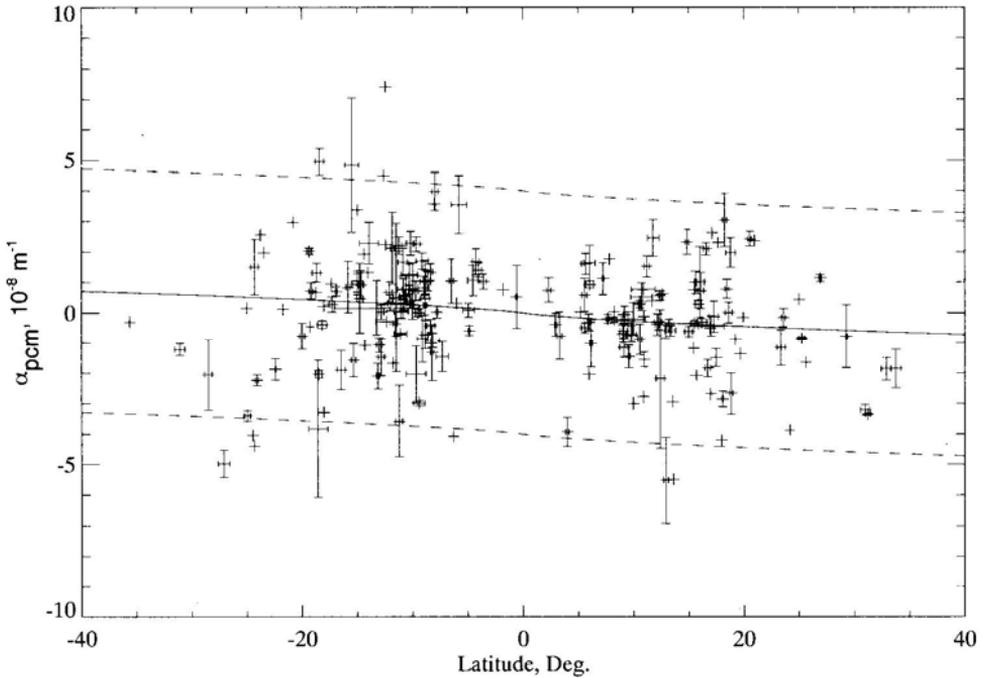
Figure 2. A measure of overall twist (α_{best}) of 203 active regions. Error bars reflect the variation in α_{best} from independent measurements of the Same active region. The mean twist predicted by a Σ-effect model is shown (solid), as well as its standard deviation (dashed), for a flux tube of $\Phi = 10^{22}$ Mx (see section 3).

The success of this simple model is striking, and its implications must be considered. Gilman & Charbonneau (1999) have shown that the creation of twist at the core-convection zone interface produces a variety of "butterfly diagrams" such as those in Fig. 3. The noteworthy aspect of these calculations is that they allow observations of the current helicity to be used to discriminate between dynamo models. However, we must ask—does the convection zone impose such a strong imprint on the current helicity of photospheric magnetic fields that it drowns out any signature of the dynamo? Longcope *et al.* (1999) argue that the amplitude of the twist generated in the dynamo region will be much less than that produced by convection zone turbulence through the Σ-effect. It remains to be seen whether any twist signature of dynamo processes at the base of the convection zone can be detected at the photosphere.

4. Evolution of magnetic helicity inside active regions

Considerable spatial variation of the current helicity is found in both solar and laboratory plasmas, and it is interesting to contrast what is known on the Sun to what has been learned from laboratory research. Studies of relaxation phenomena in laboratory plasmas show that such plasmas relax toward a minimum energy state, while keeping their relative magnetic helicity roughly constant, as originally proposed by Taylor (1974, 1986). During this evolution magnetic reconnection takes place and
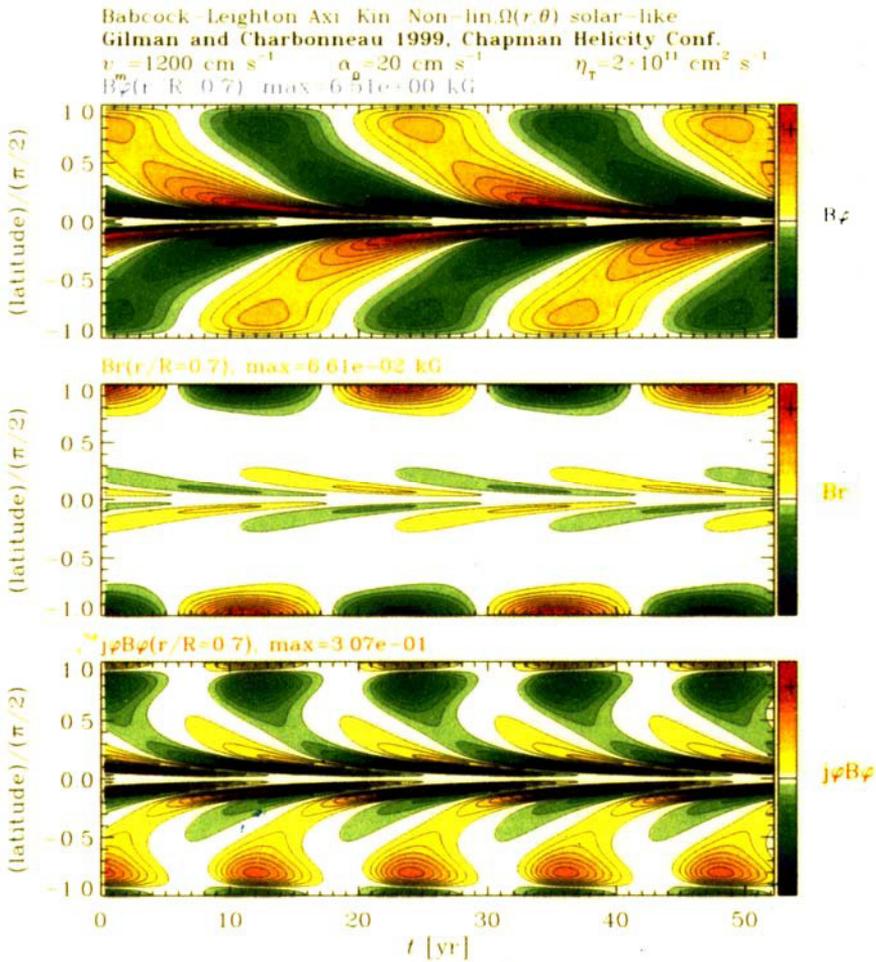
Figure 3. Butterfly diagram for the toroidal field, the radial field, and the current helicity at the interface between the core and the convection zone. Results of a model of Gilman & Charbonneau (1999), by permission.

energy is released, but magnetic helicity is much better conserved than energy (Yamada 1999).

It is well known that electric currents are nonuniform within active regions and sunspots, where they can be measured with vector magnetographs (e.g., Gary *et al.*1987). Pevtsov, Canfield & Metcalf (1994) used $\alpha_z = (\nabla \times B)_z / B_z$, as a measure of the vertical current helicity h_{cz}. They found that patches of both signs of h_{cz} are typically present inside active regions. Although these pattern evolve, individual patches can be identified for up to 4 days. Such patterns of h_{cz} were confirmed by Abramenko & Yurchishin (1996) and Wang (1999).

Though it is not understood in detail, it is plausible that local current helicity patterns will form as flux bundles rise through the convection zone. Numerical

simulations imply that structures of a given size, but opposite kinetic helicity, will form as a single magnetic flux tube bifurcates due to drag forces (Longcope, Fisher & Arendt 1996).

Bogdan (1984) found that flux tubes of the same sense of twist will merge if their relative velocities are slow enough to allow their magnetic fields to reconnect. Zweibel & Rhoads (1995) estimated an upper limit to the critical velocity and concluded that colliding twisted flux tubes may coalesce at the base of the convection zone, but not in the photosphere. In their estimate, however, they used the convective velocity for this estimate, an obvious overestimate. One might speculate that in many cases, particularly in strong field regions such as sunspots, different conclusions might result from a more exact treatment.

Pevtsov & Canfield (1999) described the evolution of the α_z-pattern late in the decay of a sunspot. Fig. 4 shows values of the cross-correlation coefficient for successive α_z-patterns inside this sunspot. The characteristic decay time of the pattern was found to be $\tau \sim 47$ hours. However, despite the presence of short term evolution, the data show no convincing indication of relaxation of the pattern towards larger spatial scales or smaller values of α_z, as we would expect from energy release and Taylor relaxation. Using Haleakala Stokes Polarimeter vector magnetograms of 18 different active regions observed for more than 8 days, we computed contours of a_z corresponding to a single fixed level $\pm 10^{-9} \mathrm{m}^{-1}$ and calculated averaged areas of patches (S_{avg}) and averaged values of α (α_{avg}) inside each patch. Fig. 5 shows the variation of α_{avg} and S_{avg} for the magnetograms observed within $\pm 45°$ of the central meridian. Despite significant scatter, the data show no systematic trend either in averaged size nor in averaged α_z.
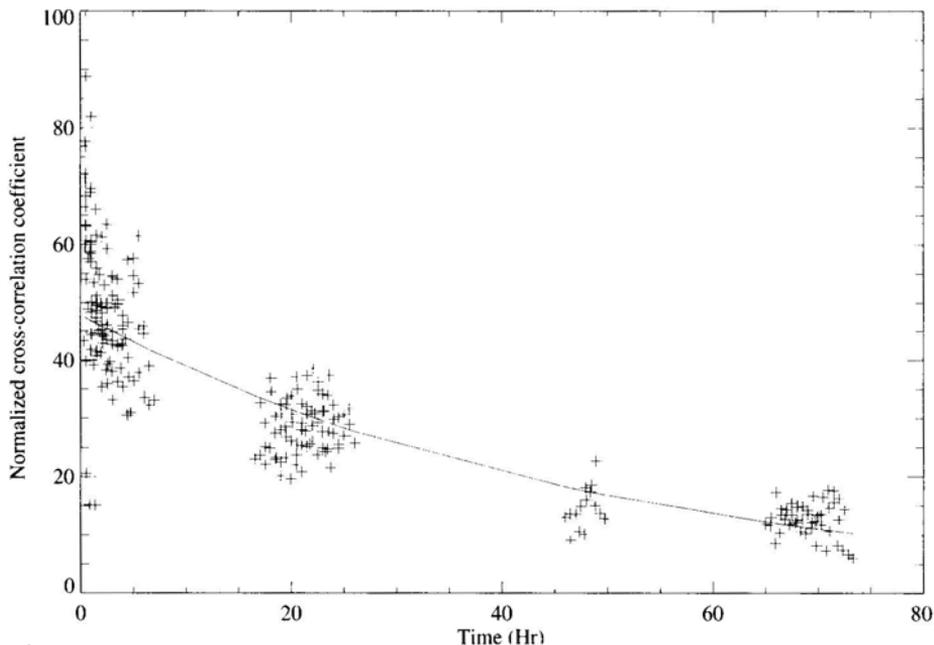

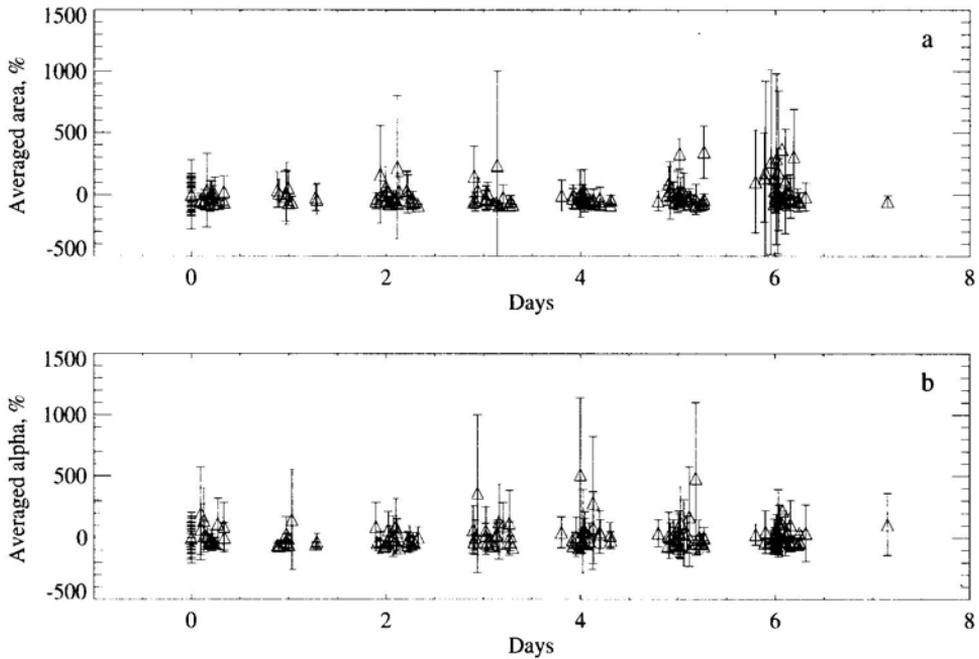**Figure 4.** Cross-correlation function computed using α-maps of decaying active region NOAA 7926.

Figure 5. Evolution of averaged size of contours corresponding to $\pm10^{-9}\text{m}^{-1}$ (**a**) and averaged value of α inside areas (**b**) for 18 active regions.

The presence of short term evolution (Fig. 4) and the lack of long-term evolution (Fig. 5) suggests to us that the local helicity pattern inside active regions evolves mostly via rearrangement of existing individual α_z patches. We see no indication of a Taylor relaxation process in our data.

References

Abramenko, V. I., Yurchishin, V..B. 1996, *Solar Phys.,* **168**, 47.
Berger, M. A. 1999, in *Magnetic Helicity in Space and Laboratory Plasmas,* (ed.) M. R. Brown, R. C. Canfield & A. A. Pevtsov, **111** of Geophys. Monogr. Ser. (Washington, D.C. AGU), 1–10.
Bogdan, T. J. 1984, *Phys. Fluids,* **27**, 994.
Caligari, P., Moreno-Insertis, F., Schüssler, M. 1995, *Astrophys. J.,* **441**, 886.
Chou, D.-Y, Fisher, G. H. 1989, *Astr. Astrophys.,* **341**, 533.
D'Silva, S., Choudhuri, A. R. 1993, *Astr. Astrophys.,* **272**, 621.
Fan, Y, Fisher, G. H., McClymont, A. N. 1994, *Astrophys. J.,* **436**, 907.
Gary, G. A., Moore, R. L., Hagyard, M. J., Haisch, B. M. 1987, *Astrophys. J.,* **314**, 782.
Gilman, P. A., Charbonneau, P. 1999, in *Magnetic Helicity in Space and Laboratory Plasmas,* (ed.) M. R. Brown, R. C. Canfield & A. A. Pevtsov, **111** of Geophys. Monogr. Ser. (Washington, D.C. AGU), 75–82.
Leka, K. D., Canfield, R. C., McClymont, A. N., Van Driel Gesztelyi, L. 1996, *Astrophys. J.,* **462**, 547.
Longcope, D. W., Fisher, G. H., Arendt, S. 1996, *Astrophys. J.,* **464**, 999.
Longcope, D. W., Fisher, G. H., Pevtsov, A. A. 1998, *Astrophys. J.,* **507**, 417.
Longcope, D. W., Klapper, I. 1997, *Astrophys. J.,* **488**, 443.

Longcope, D. W., Linton, M., Pevtsov, A. A., Fisher, G. H., Klapper, I. 1999, in *Magnetic Helicity in Space and Laboratory Plasmas,* (ed.) M. R. Brown, R. C. Canfield & A. A. Pevtsov, **111** of Geophys. Monogr. Ser. (Washington, D.C. AGU), 93–101.

Moffatt, K. H., Ricca, R. L. 1992, *Proc. R. Soc. Lond. A,* **439**, 411.

Parker, E. N. 1955, *Astrophys. J.,* **122**, 293.

Pevtsov, A. A., Canfield, R. C. 1999, in *Magnetic Helicity in Space and Laboratory Plasmas,* (ed.) M. R. Brown, R. C. Canfield & A. A. Pevtsov, **111** of Geophys. Monogr. Ser. (Washington, D.C. AGU), 103–110.

Pevtsov, A. A., Canfield, R. C, Metcalf, T. R. 1994, *Astrophys. J.,* **425**, L117.

Pevtsov, A. A., Canfield, R. C, Metcalf, T. R. 1995, *Astrophys. J.,* **440**, L109.

Spruit, H. C. 1981, *Astr. Astrophys.,* **98**, 155.

Steenbeck, M., Krause, F. 1966, *Z. Naturforsch,* **21a**, 1285.

Taylor, J. B. 1974, *Phys. Rev. Lett,* **33**(19), 1139.

Taylor, J. B. 1986, *Rev. Mod. Phys.,* **58**(3), 741.

Wang, J. 1999, *Fundamentals of Cosmic Physics,* **20**, 251.

Yamada, M. 1999, in *Magnetic Helicity in Space and Laboratory Plasmas,* (ed.) M. R. Brown, R. C. Canfield & A. A. Pevtsov, **111** of Geophys. Monogr. Ser. (Washington, D.C. AGU), 129–140.

Zweibel, E. G., Rhoads, J. E. 1995, *Astrophys. J.,* **440**, 407